Centrally Acting and Metabolically Stable Thyrotropin-Releasing Hormone Analogues by Replacement of Histidine with Substituted Pyridinium

Laszlo Prokai,*,†,‡ Katalin Prokai-Tatrai,§ Alevtina D. Zharikova,† Vien Nguyen,† Pal Perjesi,†,|| and Stanley M. Stevens, Jr.†

Department of Medicinal Chemistry, Department of Pharmacology and Therapeutics, and The McKnight Brain Institute, University of Florida, Gainesville, Florida 32610

Received November 22, 2002

Metabolically stable and centrally acting thyrotropin-releasing hormone (TRH) analogues were designed by replacing the central histidine with substituted pyridinium moieties. Their analeptic and acetylcholine-releasing actions were evaluated to assess their potency as central nervous system (CNS) agents. A strong experimental connection between these two CNS-mediated actions of the TRH analogues was obtained in subject animals. The analogue 3-(aminocarbonyl)-1-(3-[2-(aminocarbonyl)pyrrolidin-1-yl]-3-oxo-2-{[(5-oxopyrrolidin-2-yl)carbonyl]amino}propyl)-pyridinium (**1a**) showed the highest (TRH-equivalent) potency and longest, dose-dependent duration of action from a series of homologous compounds in antagonizing pentobarbital-induced narcosis when administered intravenously in its CNS-permeable prodrug form (**2a**) obtained via reduction of the pyridinium moiety to the nonionic dihydropyridine. The maximum change in hippocampal acetylcholine concentration upon perfusion of the pyridinium-containing tripeptides into the hippocampus of rats was also achieved with **1a**. No binding to the endocrine TRH receptor was measured for the TRH analogues reported here; therefore, our design afforded a novel lead for centrally acting TRH analogues. We have also demonstrated the benefits of the prodrug approach on the pharmacokinetics and brain uptake/retention of pyridinium-containing TRH analogues (measured by in vivo microdialysis sampling) upon systemic administration.

Introduction

TRH elicits a wide range of biological responses.[1] It functions as a neuroendocrine hormone by increasing TSH, leading to an elevation of thyroid hormone levels. Besides this hormonal activity, TRH has also been long recognized as a modulatory neuropeptide in the CNS[2] and has been shown to exert a variety of extrahypothalamic effects in animals. The impact of TRH on some CNS measures is associated with the augmentation of various neurotransmitter systems, mainly involving the cholinergic neurons,[3] which is independent from its hormonal activity.[4]

The best-documented effect of this small peptide is its analeptic action[5] manifested by the reduction of barbiturate narcosis or haloperidol-induced catalepsy and mediated primarily by a cholinergic mechanism.[6] TRH can also increase extracellular ACh levels, accelerate ACh turnover, improve memory and learning, and reverse the reduction in high-affinity choline uptake induced by lesions of the medial septal cholinergic neurons.[3] Therefore, this peptide has been implicated as a promising lead compound for treating motor neuron diseases,[7] spinal cord trauma,[8] and Alzheimer's disease.[9]

The use of TRH as a CNS-active agent is, however, hampered by several factors.[10] It has a short half-life after systemic administration, it does not effectively penetrate the BBB, and its endocrine effect is usually manifested at doses causing significant cognitive improvement. The poor access of TRH to the CNS is partly attributable to its low affinity to membrane lipids, which precludes an adequate BBB penetration.[11]

There have been numerous attempts to produce TRH-like compounds to separate the CNS and hormonal effects. Analogues where [His^2] is replaced by an aliphatic amino acid residue, such as by Leu or Nva, are characteristic representatives.[12] While these compounds have improved metabolic stability and somewhat higher lipophilicity compared to TRH, their peptide character still prevents them from effectively accessing the CNS.

Invasive (e.g., bypassing or altering the BBB) and noninvasive strategies[13,14] have been developed for improving CNS drug targeting of hydrophilic drugs such as neuropeptides. One of the noninvasive methods relies on the transient chemical modification(s) of the parent drug by producing lipophilic prodrugs.[14,15] Due to the improved lipophilicity, the prodrug may penetrate biological membranes including the BBB and convert to the pharmacologically active species at the site of action via predictable enzymatic and/or chemical transformation. Although the lipophilicity through prodrug creation may assure the diffusion through the BBB, efflux from the CNS is still not prevented if the prodrug → drug conversion is not adequately rapid. This problem, however, may be overcome if specific moieties, such as lipophilic dihydropyridines,[16] are used for the bioreversible alteration of the drug to produce CNS-permeable

* To whom correspondence should be addressed. Tel/fax: (352) 392-3421. E-mail: lprokai@grove.ufl.edu.
† Department of Medicinal Chemistry, College of Pharmacy.
‡ The McKnight Brain Institute.
§ Department of Pharmacology and Therapeutics, College of Medicine.
|| On leave from the University of Pécs, Hungary.

10.1021/jm020531t CCC: $27.50
Published on Web 10/12/2004

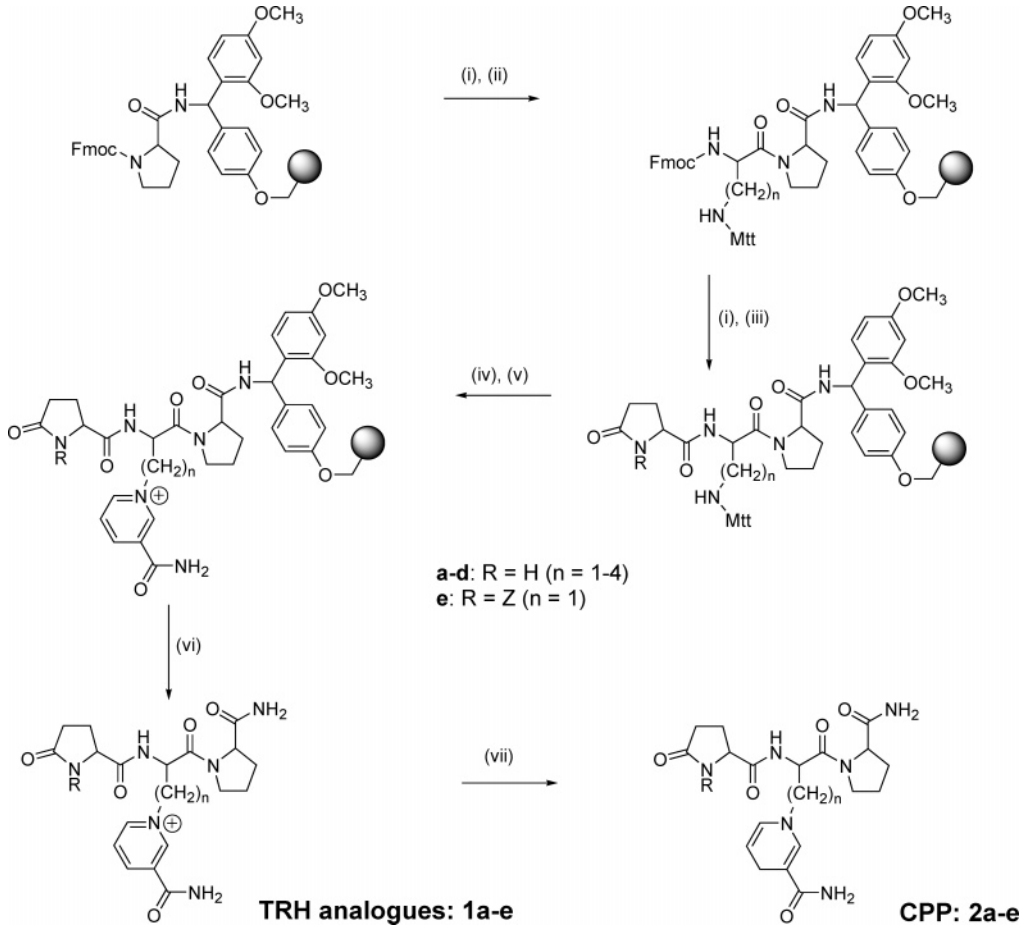

Figure 1. Synthesis of TRH analogues **1a**−**e** and their CPPs (**2a**−**e**). (i) 20% (v/v) piperidine in DMF, 10 min; (ii) PyBOP/HOBt/Fmoc-NH-CH[$(CH_2)_n$-NH-Mtt]COOH/DiPEA (1:1:1:2); (iii) PyBOP/HOBt/(Z)-pGlu/DiPEA (1:1:1:2); (iv) 1% (w/v) TFA in CH_2Cl_2, 2 × 15 min; (v) 1-(2,4-dinitrophenyl)-3-carboxamidopyridinium chloride (5 equiv), Et_3N (3 equiv), 60 °C, 5 h; (vi) TFA:H_2O (98:2, v/v); (vii) $Na_2S_2O_4$ in water, pH 7, 4 h; or polymer-supported borohydride in MeOH, 15 min (Z = benzyloxycarbonyl).

prodrugs (CPPs). Because a dihydropyridine can be converted to pyridinium in the CNS analogously to the oxidation of NAD(P)H, the obtained pyridinium−drug conjugate cannot exit the CNS by passive diffusion through the BBB. Enzymes in the brain may then remove the pyridinium moiety and, thus, liberate the drug.

Earlier we have reported[17] an enhanced delivery of a TRH analogue into the CNS that was achieved through multiple bioreversible lipidization. This rather complex strategy required, however, a cumbersome chemistry and a series of enzymatic processes for liberating the parent drug. For a simplification of this method, we designed TRH analogues with a specific moiety integrated into the structure, which would enable us to temporarily modify, without mandatory auxiliary lipophilizer(s), the peptide to furnish CNS targeting.[18] Thus, we replaced the central His, believed to be an essential structural element for the full TSH-releasing activity but not to CNS effects,[19] with pyridinium derivatives resulting in a permanent positive charge for the new tripeptides. We also hypothesized that the pyridinium moiety directly replacing the imidazole ring of His (**1a**) would yield the closest analogue of TRH and, thus, expected to emulate its CNS activity. This hypothesis was tested through the synthesis of **1a** and its side-chain-elongated homologues (**1b**−**d**) for comparison of their potency to the endogenous peptide in animal models reflecting TRH-associated pharmacological effects in the CNS.

Upon reducing the pyridinium to dihydropyridine, the resultant neutral CPPs (**2a**−**d**) should presumably reach the brain where, after oxidation, the analogues are regenerated and manifest TRH-like pharmacological activity. We also studied whether the attachment of benzyloxycarbonyl (Z) to the pGlu residue of the analogues would be appropriate for the introduction of an additional promoiety (**2e**). Here, we report the detailed evaluation of the designed TRH analogues and their CPPs as potential CNS agents.

Synthesis. The precursors of a series of TRH analogues having central substituted pyridinium moieties (**1a**−**e**, Figure 1) were prepared by semiautomated SPPS utilizing Fmoc chemistry. Introduction of the pyridinium moiety was also carried out by solid-phase Zincke reaction in DMF. In short, the preloaded Fmoc-Pro-Rink Amide-MBHA resin was deprotected with 20% (v/v) piperidine in DMF followed by coupling to the orthogonally side-chain-protected central amino acid (Dap, Dab, Orn, or Lys). Initially, we used Dde[20] side-chain protection; however, later we replaced Dde with Mtt[21] to increase the yield, because we also observed the migration of Dde to the α-amino group[22] upon Fmoc deprotection with piperidine. Once the N-terminal amino acid was attached, the Mtt was removed to unmask the side-chain amino group for the Zincke

Table 1. IAMC Capacity Factor (k'_{IAM}) and Computed Octanol/Water Partitioning (log *P*) for TRH, **1a**−**e** and **2a**−**e**

		computed log *P*		
compd	k'_{IAM}[a]	fragment based method[b]	quantum-chemical (AM1) model-based method[c]	volume-based method[d]
TRH	0.51	−4.37[e]	−0.27[e]	−1.74[e]
1a	0.30	−2.67	−2.15	−2.64
2a	0.55	−4.38	−3.14	−3.29
1b	0.42	−2.61	−1.85	−2.18
2b	0.80	−4.33	−2.92	−2.84
1c	0.49	−2.16	−2.67	−1.74
2c	1.47	−3.88	−3.30	−2.39
1d	0.60	−1.77	−2.68	−1.29
2d	2.30	−3.48	−3.55	−1.94
1e	4.37	−0.27	−6.13	−2.49
2e	11.3	−1.98	−7.26	−3.10

[a] Conditions are given in the Experimental Section (IAM chromatography). [b] Reference 26. [c] Reference 27. [d] Reference 28. [e] Experimental log *P* is −2.46 (ref 29).

reaction. We preferred solid-phase chemistry for the amine → pyridinium exchange, although solution-phase Zincke reaction was also feasible. The resin was suspended in DMF, 5 equiv of 1-(2,4-dinitrophenyl)-3-carboxamidopyridinium chloride[23] was added, and the mixture was shaken at 60 °C. The reaction was usually complete within 4−5 h (as monitored by the ninhydrin test). The novel TRH analogues were then removed from the resin using TFA/water (98:2 v/v) and purified by preparative gradient HPLC on octadecylsilica reversed phase. Identification was based on NMR, ESI-MS, and combustion analysis. For the preparation of CPPs **2a**−**e**, the pyridinium moieties were reduced with sodium dithionite[16] or polymer-supported borohydride. The progress of the reduction was monitored by HLPC and UV spectroscopy (254 nm for **1a**−**e** and 355 nm for **2a**−**e**).

Membrane Affinity. The increase in the ability of **2a**−**e** to interact with biological membranes compared to **1a**−**e** and TRH was demonstrated by immobilized artificial membrane chromatography (IAMC).[24] ESI and APCI mass spectrometries[25] were employed for detection of **1a**−**e** and **2a**−**e**, respectively. As shown in Table 1, the dihydropyridine moiety, indeed, increased membrane affinity of **2a**−**e** when compared to the corresponding pyridinium analogues **1a**−**e**. While **2a** had an IAMC capacity factor (k'_{IAM}) essentially identical to that of TRH, **2b**−**e** manifested stronger attraction to the immobilized artificial membrane than TRH. On the other hand, while the measured k'_{IAM} values show the expected tendency, the calculated log *P* values[26−28] displayed a great array of discrepancies within and among the methods employed (Table 1).

Receptor Binding. Binding affinities to the receptor were measured in pellets obtained from rat forebrain and using [^{3}H][3-Me-His^2]TRH as a radioligand. Whereas TRH inhibited radioligand binding with an inhibition constant (K_i) of 42.3 nM, K_i values of **1a**−**d** were >10 μM.

In Vitro Stability Studies. In rat plasma and brain homogenate (20% w/v), the CPPs (**2a**−**e**) converted to **1a**−**e** with half-lives ($t_{1/2}$) around 20 and 6 min, respectively (See Supporting Information, Table 1). On the other hand, TRH had $t_{1/2}$ of 16 min in brain homogenate and 11 min in plasma, while the novel analogues (**1a**−**d**) were very stable in these media (less than 10% degradation in 2 h). The longer half-lives of CPPs in plasma compared to those in brain should have a beneficial effect on CNS sequestration of the analogues after systemic administration. At the same time, the Z group on pGlu (**1e**) was quite resistant to enzymatic hydrolysis ($t_{1/2} \sim 110$ min).

Table 2. Analeptic Effects of TRH, **1a**, and **1a**−**1e** When Administered in Their CPP Forms (**2a**−**e**) at Equimolar Doses of 15 μmol/kg of Body Weight[a]

test compd	sleeping time (min ± SEM)	test compd	sleeping time (min ± SEM)
control	69.4 ± 7.9	**2b**	44.7 ± 4.7[b]
TRH	26.0 ± 3.0[b]	**2c**	58.1 ± 6.6
1a	75.9 ± 1.9	**2d**	48.8 ± 6.7[b]
2a	19.4 ± 2.1[b]	**2e**	64.5 ± 2.7

[a] Pentobarbital (ip 60 mg/kg of body weight) was injected 10 min after the iv injection of the test compounds. [b] Statistically significant difference from control ($p < 0.05$, $N = 9$−18).

Table 3. Analeptic Activities Measured at Varying Doses of **1a** When Administered in Its CPP Form (**2a**)[a]

dose (μmol/kg of body wt)	decrease in sleeping time compared to saline control (min ± SEM)
0.5	2.8 ± 1.3
1	5.4 ± 1.3
5	14.1 ± 1.6
15	23.2 ± 1.6
50	24.2 ± 2.2

[a] Pentobarbital (ip 60 mg/kg of body weight) was injected 10 min after the iv injection of the test compound.

Analeptic Activity. The antagonism of barbiturate-induced anesthesia was explored to survey the extent of activation of cholinergic neurons[6] and, thus, the potency of the new analogues as CNS agents administered iv (in their CPP forms) to the animals. The vehicle alone (1.5 mL/kg of body weight) or equimolar doses (15 μmol/kg of body weight) of test compounds (**1a**, **2a**−**e**, and TRH) were injected through the tail vein of the mice. After 10 min, each animal received an ip injection of sodium pentobarbital at a dose of 60 mg/kg of body weight. The sleeping time was recorded from the onset of the loss of righting reflex until the reflex was regained. As shown in Table 2, a significant decrease in the sleeping time was achieved by prodrugs **2a**, **2b**, and **2d** compared to the control. The most potent prodrug **2a** was essentially equipotent with TRH when the cholinergic challenge was done 10 min after drug administration, and the action was dose dependent (Table 3). However, its further lipophilized form **2e** was inactive in this pharmacological paradigm. Consequently, a free pGlu appears to be an essential feature of the design to produce analeptic activity. On the basis of the observed brain homogenate half-life of **1e** ($t_{1/2} \sim$ 110 min), we concluded that the actual active analogue **1a** could not be formed in the brain rapidly enough from **1e.** As expected, **1a** was ineffective when administered iv without transformation to prodrug form, due to its inability to sufficiently penetrate the CNS (see Table 2).

The prodrug **2a** was further studied and compared to TRH with respect to duration of analeptic action by increasing the time at which the animals were challenged with barbiturate injection (Figure 2) after pretreatment with TRH or **2a**. The analeptic effect of TRH showed an overall decrease, when the time between

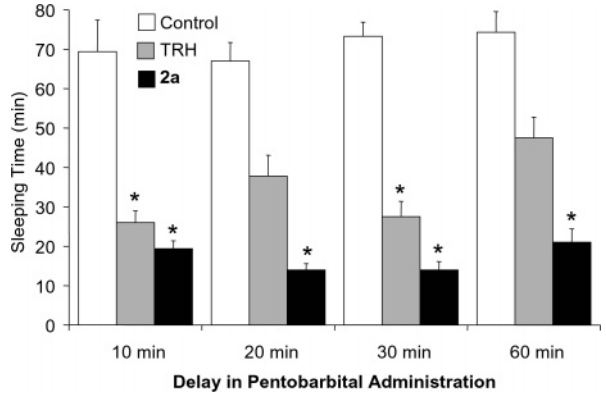

Figure 2. Duration of analeptic action of TRH and **2a** at equimolar dose (15 μmol/kg of body weight, iv) upon varying the time (10, 20, 30, and 60 min) for pentobarbital post-administration (ip, 60 mg/kg of body weight). Asterisks indicate statistically significant differences (ANOVA followed by post hoc Dunnett's test, $p < 0.05$) compared to control.

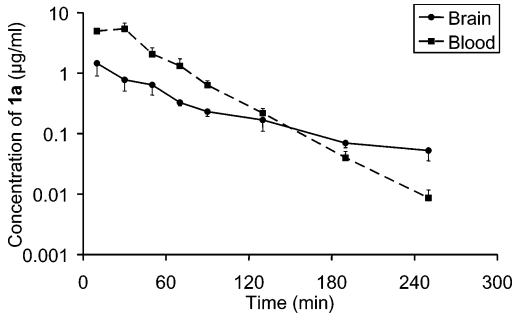

Figure 3. Concentration of TRH analogue **1a** in the hippocampus (circles, solid line) and in blood (squares, dashed line) of rats, measured via in vivo microdialysis sampling followed by LC/ESI-MS/MS assay, after ip injection of its prodrug **2a**.

Table 4. Maximal Changes in Hippocampal ACh Concentration When TRH and Its Analogues **1a**−**d** Were Perfused (1 nmol/μl Solutions at 2 μL/min) through a Microdialysis Probe Placed into the Hippocampus of Rats[a]

test compd	ACh concn (% basal level ± SEM)	test compd	ACh concn (% basal level ± SEM)
control	120 ± 15	**1b**	216 ± 11[b]
TRH	394 ± 14[b]	**1c**	145 ± 7
1a	279 ± 10[b]	**1d**	242 ± 10[b]

[a] Values expressed as percentages of the ACh concentration measured before perfusion of the test compounds (baseline; average of three analyses from successive 20-min fractions). [b] Statistically significant difference ($p < 0.05$) from control.

injections was increased. A loss of over half of the analeptic effect was observed upon injecting pentobarbital 60 min after the administration of TRH, when compared to pentobarbital injection after 10 min. Upon pretreatment with **1a** (formed in the CNS from **2a**), analeptic activity actually reached its highest point after 20−30 min, and a near-maximal effect was maintained even when the barbiturate challenge was delayed by 60 min.

Effect on ACh Release. This study was devoted to a comparative evaluation of **1a**−**d** and TRH by measuring the changes in hippocampal ACh concentration when the compounds were perfused through a microdialysis probe placed into the hippocampus of rats.[30] Values shown in Table 4 are expressed as percentages of the ACh concentrations measured before the perfusion with the solutions containing **1a**−**d**, respectively. Although none of the analogues outperformed TRH in this experimental model, **1a**, **1b**, and **1d** significantly increased ACh levels compared to control. The most potent analogue (**1a**) showed an approximately 30% lower stimulation of the ACh release than TRH. Thus, the latter neurochemical effect gave the same tendency upon increasing the length of the side chain (**1a** → **1d**) as observed for the analeptic action.

Pharmacokinetics and Brain Uptake/Retention. To assess the benefits of brain-targeting by the CPP approach, concentrations in the brain and blood for the most potent analogue (**1a**) were measured after the ip injection of **2a** (15 mg/kg body weight) to rats. Sample collection was done by in vivo microdialysis[31] from the extracellular space of the hippocampus and from the jugular vein, and HPLC/ESI-MS/MS analyses were performed to measure the concentrations of **1a**. As shown in Figure 3, both the hippocampus and blood concentrations of the TRH analogue reached their maxima within 30−50 min. The measured highest extracellular level of **1a** in the hippocampus was about 3−4-fold lower than its concentration in the blood; the first-order rate constant for the subsequent elimination of **1a** from the systemic circulation (1.62 h^{-1}) was, however, about 3-fold higher than that from the specified CNS location (0.59 h^{-1}). Therefore, the concentration of the TRH analogue in the hippocampus and in the blood became equal around 120−150 min, and the CNS level of **1a** was considerably (about 6-fold) higher than its concentration in the systemic circulation 4 h after ip administration of its CPP (**2a**).

Discussion

Degradation-resistant and centrally acting TRH analogues (**1a**−**d**) were obtained by replacing the central His with amino acids having a 3-carboxamido-1-pyridylalkyl side chain derived synthetically via a solid-phase Zincke reaction from Dap, Dab, Orn, and Lys precursors, respectively. The replacement of His practically abolished the endocrine activity of these analogues on the basis of the greatly diminished binding affinity to the receptor labeled by [^{3}H][3-Me-His^2]TRH. The pyridinium moiety also allowed us to perform a simple and bioreversible chemical modification (reduction) of **1a**−**e** to produce CPPs (**2a**−**e**). Conversion of the ionic, membrane-impermeable pyridinium analogues of TRH to the corresponding dihydropyridines produced neutral, nonionizable compounds, thereby not only facilitating their passive diffusion through the BBB but also inhibiting CNS efflux due to enzymatic oxidation to the (pharmacologically active) pyridinium form within the brain (see Figure 3).

Calculated log *P* values used extensively in earlier studies to rationalize CNS delivery[16] were uninterpretable for the compounds involved in this study. One expects an increase in the lipophilicity upon making dihydropyridines out of pyridinium compounds;[16] yet log *P* data obtained by calculations (Table 1) consistently predicted the pyridinium compounds (**1a**−**e**) to be significantly more lipophilic than the corresponding 1,4-dihydropyridines (**2a**−**e**). Therefore, the predictive power of current in silico methods to aid the design of CNS-bioavailable agents from neuropeptides based on the principle employed in this study appears to be unreli-

able at best. [A fairly straightforward yet somewhat arbitrary adjustment of the calculated lipophilicities by using the 1.91 log unit difference between the computed and experimental log P (−2.46)[29] values of TRH as a correction factor applied to the prodrugs *only*, which affords log P values of −2.47, −2.42, −1.97, −1.57, and −0.07 for **2a**−**e**, respectively, emerges to fix the problem for the values obtained by the atom fragment method[26] and listed in the third column of Table 1; however, such an uncomplicated correction of the computed lipophilicities could not be employed for the other two in silico methods.[27,28]] On the other hand, IAMC has furnished readily interpretable data.

The measured k'_{IAM} chromatographic capacity factors clearly and consistently showed the enhanced lipid membrane affinity of the prodrugs compared to the TRH analogues reported here (Table 1). IAMC assesses affinity to monolayers of cell membrane phospholipids immobilized by covalent binding on silica particles and mimics membrane interactions better than partitioning in the isotropic *n*-octanol/water system. This chromatographic technique has been applied for the prediction of penetration across the BBB for HIV protease inhibitors,[32] steroids,[33] and biogenic amines.[33] The k'_{IAM} obtained for a compound is directly related to its partition coefficient between the aqueous phase and the chemically bonded membrane phase and, ultimately, to the K_m value representing its fluid membrane partition coefficient.[24] However, while there is a widely accepted "reference point" (log $P = 2 \pm 0.5$)[34] for an optimum transport across the BBB by diffusion upon using *n*-octanol/water partitioning, k'_{IAM} values are relative to reference compounds that show no affinity to lipid membranes (e.g., citric acid used in this study). From the IAM chromatographic measurements, an indication to the extent of BBB permeability of the prodrugs (**2a**−**e**) was obtained by predicting brain uptake indices (BUIs) based on the reported correlation[33] between the (log BUI)($\sqrt{}$MW) values,[35] where MW is the molecular weight, and the log k'_{IAM} values using six drugs (tryptophol, nicotine, dopamine, epinephrine, norepinephrine, and aspirin) in a "training set" to establish the regression (see Supporting Information, Table 2). The lowest k'_{IAM} of 0.55 and the highest k'_{IAM} of 11.3 translated to BUIs of about 4% (which was practically identical to that of TRH) and 11% for **2a** and **2e**, respectively. However, BUIs reflect BBB permeability after a single capillary transit, and the actual brain uptakes were apparently higher (Figure 3) due to circulation and because of the "sink" created by the metabolic conversion of the neutral CPP to the ionic, membrane-impermeable pyridinium compound in the CNS.

While **1a** was essentially equipotent with TRH (Table 2) and manifested dose dependence (Table 3) when administered in its CPP form (**2a**) in reducing pentobarbital-induced sleeping time, it was ineffective without the transient chemical alteration when injected into the tail veins of mice. It could also be concluded that the amide hydrogen of the pGlu residue was necessary for achieving analeptic activity with our design and modification of the pGlu residue with benzyloxycarbonyl (Z) did not afford a prodrug.

The analogues were very stable in biological media; accordingly, a long-lasting analeptic activity was observed (Figure 2). We have also demonstrated the benefits of the CPP approach on the brain uptake/retention and pharmacokinetics of pyridinium-substituted TRH analogues (Figure 3).

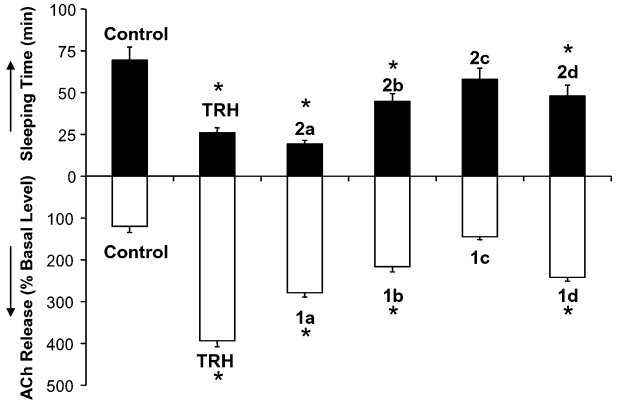

Figure 4. Parallel trends of analeptic and ACh-releasing activities of the novel TRH analogues in rats, together with those of TRH, at equimolar doses [15 μmol/kg of body weight, iv, as CPPs, and perfusion of the pyridinium compounds (1 nmol/μL solution at 2 μL/min) into the hippocampus by microdialysis, respectively]. Asterisks indicate statistically significant differences (ANOVA followed by post hoc Dunnett's test, $p < 0.05$) compared to control.

Central ACh-releasing activity of the new analogues was also studied in a rat model. The results showed the same trend for **1a**−**d** (Table 4) as observed for the analeptic effect after systemic administration of the corresponding CPPs (Table 2). The analogue having the shortest side chain in the central residue (**1a**) produced the highest change in the hippocampal ACh concentration compared to control.

In both experimental models, statistically significant effects compared to control were achieved, with the exception of **1c**, indicating the strong connection between analeptic activity and ACh-releasing capacity of TRH analogues (Figure 4). However, side-chain elongation resulted in a V-shape profile of the pharmacological responses; i.e., adding one (**1b**) and two additional methylene groups (**1c**) into the side chain of the central residue gradually abolished potency compared to **1a**, but the addition of a third methylene (**1d**) restored potency to some extent (Figure 4). This trend has remained to be explored and, perhaps, exploited in a future study. Altogether, **1a** may be considered as a novel type of lead for centrally acting TRH analogues.

Experimental Section

Instruments, Materials, and Methods. All chemicals used were reagent grade or peptide synthesis grade. Solvents were obtained from Fisher Scientific (Atlanta, GA). TRH, Fmoc-Pro-Rink-MBHA resin (loading: 0.5 mmol/g), and amino acids were purchased from Bachem BioSciences (Torrance, CA). ACh was purchased from Sigma (St. Louis, MO). Polymer-supported (Amberlyst A-26) borohydride (loading: 2 mmol/g BH_4) was purchased from Aldrich Chem. Co. (Milwaukee, WI). UV spectra were recorded in MeOH on a Cary 3E UV−visible spectrophotometer (Varian, Walnut Creek, CA). A Synthor 2000, Peptide International (Louisville, KY) instrument was used for the preparation of the individual peptides by Fmoc chemistry. The peptides were purified on a preparative RP-HPLC system consisting of a Thermo Separations (Fremont, CA) SpectraSERIES P200 binary gradient pump (operated at 5 mL/min), a Rheodyne (Cotati, CA) model 7125 injector valve equipped with a 5 mL loop, and a Spectra 100 UV/vis detector

set at 216 nm. Analytical HPLC (1 mL/min flow rate) was done on a Surveyor HPLC system operated by ChromQuest 4.0 chromatography workstation software (Thermo Finnigan, San Jose, CA). The semipreparative (250 mm × 10.0 mm i.d., C18) and analytical (150 mm × 4.6 mm i.d., Econosil C18) reversed-phase columns were obtained from Vydac (Hesperia, CA) and Phenomenex (Torrance, CA), respectively. The mobile phases were mixed from 0.1% (v/v) TFA (solvent A) in H_2O and 0.08% (v/v) of TFA in CH_3CN (solvent B), and gradient elution (from 5 to 35% B in 30 min) was used. Depending on the ionization amenability of the analyte, ESI or APCI ionization methods were employed for the compounds reported here. Mass spectra were obtained by a quadrupole ion trap instrument (LCQ, Thermo Finnigan, San Jose, CA) equipped with Xcalibur v1.3 software. Full-scan mass spectra were acquired from *m/z* 200 to 800 using the automatic gain control mode of ion trapping. Accurate mass measurements were obtained by a Bruker (Billerica, MA) FT-ICR mass spectrometer (BioApex 4.7e) equipped with a 4.7-T passively shielded superconducting magnet and coupled to a modified (heated metal capillary) Analytica (Branford, CT) ESI source. High-resolution mass spectra were obtained by collecting 8K time domain signals over a 5 kHz frequency bandwidth. Thirty-two time domain signals were co-added prior to Fourier transform. ^{1}H NMR spectra were recorded on Bruker AVANCE instruments (Bremen, Germany). Resonance frequency was 500 MHz. Atlantic Microlab, Inc. (Norcross, GA) performed the combustion analyses. Satisfactory C, H, N analyses were obtained for the novel compounds reported here.

3-(Aminocarbonyl)-1-(3-[2-(aminocarbonyl)pyrrolidin-1-yl]-3-oxo-2-{[(5-oxopyrrolidin-2-yl)carbonyl]amino}-propyl)pyridinium Trifluoroacetate (1a). SPPS utilizing standard Fmoc chemistry with PyBOP/HOBt/ DIPEA (1:1:2) activation on a semiautomated peptide synthesizer was used. The synthesis started with Fmoc-group removal of the preloaded Fmoc-Pro-Rink-MBHA-Amide resin with 20% (v/v) piperidine in DMF for 10 min. The orthogonally protected *N*-α-Fmoc-*N*-*β*-4-methyltrityl-diamonipropionic acid (Fmoc-Dpr(Mtt)-OH) was used to introduce the precursor of the central amino acid. After linking the N-terminus with pGlu, the Mtt protecting group was removed with 1% TFA (v/v) in CH_2Cl_2 (2 × 15 min). Then the resin was suspended in DMF (1 g/30 mL), and 5 equiv of 1-(2,4-dinitrophenyl)-3-carboxamidopyridinium chloride was added together with 3 equiv of triethylamine. The reaction mixture was agitated at elevated temperature (60 °C). The progress of the Zincke reaction was monitored by ninhydrin test and/or ESI-MS after cleaving a small amount of peptide from a tiny amount of beads. The color change of the solvent (from red to yellow) could be used as an indicator for the product formation. Upon completion of the amine → pyridinium exchange, the resin was thoroughly washed with MeOH, DMF, and CH_2Cl_2. The product was removed from the solid support by TFA/water (98:2 v/v, 1 g of resin/10 mL, 4 h). A nitrogen stream was used to concentrate the solution. The oily residue was washed several times with diethyl ether, and the solid obtained was subjected to RP-HPLC purification. After freeze-drying the combined chromatographic fractions containing **1a**, the purity of the product was verified by combustion analysis. Identification was based on MS and ^{1}H NMR spectroscopy. Peptides **1b**−**e** were synthesized, purified, and identified analogously. For **1e**, Z-pGlu was used instead of pGlu for terminating the peptide chain. White, hygroscopic solid: yield 24%; MS (ESI) *m/z* 417 (C^+); HRMS (ESI) found *m/z* 417.1889, calcd *m/z* 417.1868; ^{1}H NMR [H_2O/D_2O (8:2 v/v)] tentative assignment for the major (>90%) rotamer,[36] *δ* (ppm) 9.22 (s, 1H, pyridinium H-2); 8.95 (d, J = 6.18 Hz, 1H, pyridinium H-6), 8.23 (d, J = 8.84 Hz, 1 H, pyridinium H-4), 8.09 (dd, J = 8.27 and 6.21 Hz, 1H, pyridinium H-5), 8.48 (bs, 1H, pGlu-NH), 6.95 (bs, Pro-$CONH_2$), 5.26 (dt, 1H, J = 8.26 and 3.1 Hz, H-*β* of central residue), 5.07 (dd, 1H, J = 8.61 and 5.16 Hz, H-*β* of central residue), 4.56 (unresolved multiplet, 1 H, H-α of central residue), 4.31 (dd, J = 8.67 and 4.14 Hz, 1H, Pro α-H), 4.19 (dd, J = 4.22 Hz, 1H, pGlu α-H), 3.52−3.48 (m, 1H), 3.41−3.37 (m, 1H), 2.44−2.40 (m, 1H), 2.23−2.14 (m, 3H), 1.91−1.83 (m, 3H), 1.68−1.79 (m, 1H). Anal. ($C_{21}H_{25}N_6O_7F_3 \cdot 2CF_3COOH \cdot H_2O$): C, H, N.

1-(3-[2-(Aminocarbonyl)pyrrolidin-1-yl]-3-oxo-2-{[(5-oxopyrrolidin-2-yl)carbonyl]amino}propyl)-1,4-dihydropyridine-3-carboxamide (2a). Under continuous nitrogen atmosphere, **1a** (15 mg, 0.02 mmol) was dissolved in 50% (v/v) aqueous MeOH (1 mL) and then sodium dithionite[16] (10 equiv) was added together with enough sodium bicarbonate to adjust the pH to 6.5−7.0. The progress of the reduction was monitored by UV spectrophotometry (355 nm) and MS. Once the reduction was completed (usually within 2 h), the reaction mixture was extracted (3×) with cold, degassed CH_2Cl_2 (1 mL). The solvent was then removed in vacuo. Pale yellow semisolid: yield 65%; MS (APCI) *m/z* 419 $[M + H]^+$; UV_{max} 355 nm; ^{1}H NMR (DMSO-d_6) typical resonances for the CPP, *δ* (ppm) 7.13 (d, 1H, J = 1.6 Hz, dihydropyridine H2), 5.95 (dd, 1H, J = 8.06 and 1.6 Hz, dihydropyridine H6), 4.91−4.84 (unresolved m, 1H, dihydropyridine H5), 3.01−2.95 (unresolved m, 2H, dihydropyridine H4). Anal. ($C_{19}H_{26}N_6O_5 \cdot 3H_2O$): C, H, N.

(A very rapid reduction of the pyridinium moiety could be carried out with polymer-supported borohydride; 0.25 equiv of hydride in the form of borohydride-resin was added to 1 equiv of peptide dissolved in degassed MeOH under a nitrogen stream and ice cooling. The reduction was complete within 10−15 min according to UV and MS reaction monitoring. The resin was filtered off, and the solvent was blown away with a nitrogen stream. The workup was analogous with that following dithionite reduction.)

IAM Chromatography. A 3 cm × 4.6 mm i.d. IAM.PC.DD2 column (Regis Technologies, Morton Grove, IL) was employed. An isocratic solvent delivery (10 mM ammonium acetate adjusted to pH 5.4 with acetic acid) of 1.0 mL/min was provided by a SpectroFlow 400 HPLC pump (Kratos Analytical, U.K.), and APCI-MS detection was used.[30] IAM capacity factors (K'_{IAM}) were calculated as follows: $k'_{IAM} = (t_{R(X)} - t_{R(citric\ acid)})/t_{R(citric\ acid)}$, where $t_{R(X)}$ and $t_{R(citric\ acid)}$ are the retention times for the compound of interest and the void volume marker (citric acid), respectively.

Radioligand Binding. Competitive binding to TRH receptors was measured in the rat forebrain membrane using [^{3}H][3-Me-His^2]TRH as a radioligand by NovaScreen (Hannover, NJ) according to published methods.[37] Briefly, a suspension of the membrane (in 20 mM phosphate buffer, pH 7.4) was incubated with the radioligand (2 nM) and varying concentrations of the TRH analogue at 4 °C for 180 min. Nonspecific binding was measured by adding 10 μM TRH (K_i = 42.3 nM).

In Vitro Metabolic Stability Studies. Stability studies were performed in rat brain homogenate and plasma. Approximately 100 nmol of test compound was added to 1 mL of rat plasma or brain homogenate (20% w/w, 0.1 M phosphate buffer, pH 7.4), and the mixture was incubated at 37 °C in a temperature-controlled, shaking water bath. Aliquots (100 μL) were removed after 2, 5, 15, 30, 45, 60, and 90 min of incubation and transferred into a 1.5-mL Eppendorf tube containing 200 μL of ice-cold solution of 5% (v/v) acetic acid in acetonitrile. The samples were centrifuged and the supernatant was removed and analyzed by HPLC to monitor the decline in the concentration of the compound added. Standards for the assay calibration were made by adding analytes (after serial dilutions from a stock solution) into denatured tissue homogenate and plasma (at 90 °C for 30 min), respectively.

Animals. Swiss Webster mice (30 ± 2 g body weight) were used for the analeptic experiments. ACh release, pharmacokinetics, and brain uptake/retention were studied in male Sprague−Dawley rats (250−300 g body weight). The animals were purchased from Harlan (Indianapolis, IN). All animal experiments were conducted in accordance with the guidelines set forth in the Declaration of Helsinki and the Guiding Principles in the Care and Use of Animals (DHEW Publication, NIH 80-23).

Analeptic Activity. We adapted a paradigm reported in ref 5a. Eight to sixteen mice were used in each group. Test compounds were dissolved in degassed saline. The vehicle

alone (1.5 mL/kg of body weight) was administered to the animals in the control group. Equimolar doses of test compounds (15 μmol/kg of body weight) were injected through the tail vein. After 10 min, each animal received an ip injection of sodium pentobarbital solution (50 mg/mL) at a dose of 60 mg/kg of body weight. The sleeping time was recorded from the onset of loss of the righting reflex until the reflex was regained.

Effect on Extracellular ACh Levels. Our assay relied on the simultaneous delivery of the experimental agent and sampling of the extracellular space of the brain via in vivo cerebral microdialysis.[29] First, the implantation of a cerebral guide cannula (CMA/Microdialysis, Inc., Acton, MA) into the rat was done stereotaxically by using a frame equipped with a micromanipulator under aseptic conditions after the animal had been completely anesthetized (sodium pentobarbital, 50 mg/kg ip). The top of the head was shaved, and a midline cut was made through the skin. Fascia over the skull was scraped away, and the cut was protracted. With a hand-held dental drill, one hole was drilled through the skull, one at 1.4 mm to the right of the superior sagittal sinus for the guide cannula, and two additional holes were made posterior to this hole for the anchor screws. Target site for the guide cannula was the ventral hippocampus (A, −6.0 mm; L:, −4.9 mm; V, −3.5 mm). The guide cannula was held permanently in place with cranioplastic cement filling the protracted area. The actual process of insertion of the probe into the hippocampus started after allowing 7 days for the wound to heal following the implantation of the guide. After inserting the microdialysis probe into the guide and connecting the tubing for the influx and efflux of the perfusion fluid, the animal was placed into a clear plastic bowl equipped with a balanced arm for keeping the tubing away from the animal during the experiment. The animal was sacrificed after the microdialysis experiment, and the placement of the probe was verified by histological observation.

Concentric microdialysis probes (CMA/12, CMA/Microdialysis, Inc., Acton, MA) with a 4-mm-long polycarbonate membrane (cutoff molecular weight 20000) were used. An artificial cerebrospinal fluid (147 mM Na^+, 4 mM K^+, 155 mM Cl^-, and 2.4 mM Ca^{2+}) containing 2 μM neostigmine was employed as a perfusion medium. Syringe pumps (1 mL BeeStinger), their controller (BeeKeeper), and a refrigerated fraction collector (HoneyComb) used throughout the experiments were purchased from BAS (West Lafayette, IN). After a 3-h perfusion of the probes at 2 μL/min with the artificial CSF containing 2 μM neostigmine, three 20-min fractions were collected to obtain the baseline ACh concentration. For measuring the effect of the test compounds on extracellular ACh level after direct delivery into the selected tissue site via the probe, TRH and **1a**−**d**, respectively, were dissolved in the perfusion fluid at 1 nmol/μL concentration, and the probe placed in the hippocampus was perfused with these solutions, respectively, for 3 h while microdialysates were collected in 20-min fractions. A manual valve (CMA/110, CMA/Microdialysis, Inc., Acton, MA) was used for switching perfusion solutions without the interruption of the flow through the probe.

The system for the analysis of ACh in the microdialysates consisted of an MF-8500 solvent degassing unit, a PM-80 pump, a CC-5 injector with a 5-μL loop, a 50 cm × 1.0 mm i.d. MF-8904 microbore ion-exchange chromatography (IEC) column, a 2 cm × 1.0 mm MF 8903 microbore immobilized enzyme reactor (IMER), and an LC-4C electrochemical (amperometric) detector (all purchased from BAS, Inc., West Lafayette, IN). A CC-5 flow cell containing a peroxidase redox polymer coated on the glassy carbon electrode was used, and the working potential against the Ag/AgCl reference electrode was +100 mV. The mobile phase (50 mM K_2HPO_4 buffer, pH 8.5, containing 0.005% Kathon CG) was delivered at a flow rate of 130 μL/min. A PeakSimple chromatographic data system (SRI, Menlo Park, CA) was used for data acquisition and processing. Standards for assay calibration were made by serial dilutions of an ACh stock solution with artificial cerebrospinal fluid. The average of the ACh concentrations measured in the three 20-min fractions collected before starting the perfusion of the probe with the solution of the TRH analogue was considered the baseline value.

Brain and Blood Concentration Measurement. In vivo cerebral microdialysis sampling from the hippocampus was performed similarly to that described in the above section, with exception that perfusion on the probes were done at 1 μL/min with artificial cerebrospinal fluid only during sample collection. Additionally, another microdialysis probe was implanted under anesthesia into the jugular vein of the animal on the day of the experiment for a simultaneous microdialysis sampling from the blood by perfusion of the probe with an anticoagulant solution (3.5 mM citric acid, 7.5 mM sodium citrate, and 13.5 mM dextrose) at 1.0 μL/min. After the animal recovered from anesthesia, the probes were attached to separate syringe pumps and the probes were equilibrated by perfusion for 1 h, followed by a 1.5-h perfusion with solutions of **1a** (1 μg/mL). After a 30-min delay from the start of the perfusion of the TRH analogue, three 20-min fractions were collected for the subsequent determination of probe permeabilities ("recoveries"), respectively. Then, perfusion of the cerebral and vascular probes with artificial cerebrospinal fluid and anticoagulant solution was resumed for 2 h, when **2a** (15 mg/kg of body weight; 100 μL of saline vehicle) was injected by the ip route. After a delay time equivalent to the dead volume of the sampling system, 20-min fractions (20 μL each) were collected for 280 min. The first five fractions were analyzed individually, while three fractions respectively between 100 and 160, 160−220, and 220−280 min were pooled before the LC/ESI-MS/MS assay.

Five microliters of the microdialysis samples was spiked with internal standard (**1d**, 1 ng/μL) and loaded onto a microbore reversed-phase HPLC column (5 cm × 0.5 mm i.d. Targa C18, Higgins Analytical, Mountain View, CA) column using a Surveyor autosampler (ThermoFinnigan, San Jose, CA) equipped with a 10-μL sample loop. The autosampler valve was operated in combination with a MicroPro solvent delivery system (Eldex Laboratories, Napa, CA) supplying an isocratic flow (10 μL/min, 8% acetonitrile/0.5% acetic acid) to the analytical column. The eluate from the analytical column was directed to waste for 4 min via a divert valve incorporated into the mass spectrometer, which allowed for in-line sample desalting. Then, a change in divert valve configuration allowed the eluate from the HPLC column to enter into the mass spectrometer. ESI experiments were performed on a quadrupole ion trap instrument (LCQ, specified in the Instruments, Materials, and Methods paragraph). ESI spray voltage and capillary temperature were maintained at 4.5 kV and 200 °C, respectively, using a sheath gas flow of 70 arbitrary units to aid in desolvation. Product ion mass spectra were acquired in selected-reaction monitoring (SRM) mode of operation with automatic gain control mode of ion trapping disabled (targeted ions were allowed to accumulate in the trap for 300 ms). The SRMs used the two most abundant CID product ions of the analyte (**1a**, *m/z* 417 → 295, 250) and the internal standard (**1d** *m* / z 459 → 345, 223) for quantitative analysis. Standards for the assay calibration were made by serial dilutions from a stock solution of the analyte with artificial cerebrospinal fluid and anticoagulant solution, respectively. The measured concentrations of **1a** in the microdialysates were converted to tissue concentrations by division with the respective fractional recovery factor (FRF) of the probe. FRF was obtained as $(c_{in} - c_{out})/c_{in}$, where c_{in} was the concentration of **1a** entering into the probe (1 μg/mL) and c_{out} was its concentration measured in the efflux based on the analysis of the three 20-min microdialysis fractions collected during the probe-permeability-determination phase of the experiment.

Statistical Analysis. Treatment of data was done by analysis of variance (ANOVA) followed by post hoc Dunnett's test for comparison to the control group, or Tukey test upon comparing multiple means. Differences were considered significant when $p < 0.05$.

Acknowledgment. The authors thank the National Institutes of Health (MH59380) for financial support

and Tamara Blagojevic, April C. Braddy, and James R. Rocca for valuable contributions.

Appendix

Abbreviations. ACh, acetylcholine; APCI, atmospheric-pressure chemical ionization; BBB, blood−brain barrier; BUI, brain uptake index; CNS, central nervous system; CPP, CNS-permeable prodrug; Dab, 2,4-diaminobutyric acid, Dap, 2,3-diaminopropionic acid; Dde, (1-(4,4-dimethyl-2,6-dioxocyclohex-1-ylidene)ethyl); DIPEA, *N*,*N*-diisopropylethyl amine; DMF, *N*,*N*-dimethylformamide; ESI, electrospray ionization; Fmoc, 9-fluorenylmethyloxycarbonyl; His, histidine; ip, intraperitoneal; iv, intravenous; Leu, leucine; log *P*, logarithm of *n*-octanol/water partition coefficient; Mtt, (4-methyltrityl); Nva, norvaline; pGlu, pyroglutamic acid; Pro, proline; PyBOP, benzotriazole-1-yl-oxy-trispyrrolidinophosphonium hexafluorophosphate; SPPS, solid-phase peptide synthesis; TSH, thyrotropin-stimulating hormone; TRH, thyrotropin-releasing hormone; Z, benzyloxycarbonyl.

Supporting Information Available: In vitro stability of the compounds, prediction of BUIs of TRH and **2a**−**e** from their IAM chromatographic capacity factors (k'_{IAM}), and combustion analyses. This material is available free of charge via the Internet at http://pubs.acs.org.

References

(1) Horita, A.; Carino, M. A.; Lai, H. Pharmacology of Thyrotropin Releasing Hormone. *Annu. Rev. Pharmacol. Toxicol.* **1986**, *26*, 311−332.

(2) Prokai, L. Central Nervous System Effects of Thyrotropin-Releasing Hormone and Its Analogues: Opportunities and Perspectives for Drug Discovery and Development. In *Progress in Drug Research;* Jucker, E., Ed.; Birkhäuser Verlag: Basel, 2002; Vol. 59, p 133.

(3) (a) Yarbrough, G. G. TRH Potentiates Excitatory Actions of Acetylcholine on Cerebral Cortical-Neurons. *Nature* **1976**, *263*, 523−524. (b) Yarbrough, G. G. Thyrotropin Releasing Hormone and CNS Cholinergic Neurons. *Life Sci.* **1983**, *33*, 111−118.

(4) Stwertka, S. A.; Vincent, G. P.; Gamzu, E. R.; MacNeil, D. A.; Vederese, A. TRH Protection Against Memory Retrieval Deficits Is Independent of Endocrine Effects. *Pharmacol. Biochem. Behav*. **1991**, *41*, 145−152.

(5) (a) Breese, G.; Cott, J.; Cooper, B.; Prange, A.; Lippton, M.; Plotnikoff, N. Effect of Thyrotropin-Releasing Hormone (TRH) on Actions of Pentobarbital and Other Centrally Acting Drugs. *J. Pharmacol. Exp. Ther.* **1975**, *193*, 11−22. (b) Horita, A.; Carino, M.; Lai, H. Analeptic Activity Produced by TRH Microinjection into Basal Forebrain Area in the Rat. *FASEB J*. **1986**, *45*, 795. (c) Horita, A.; Carino, M.; Smith, J. Effects of TRH on the Central Nervous System of Rabbit. *Pharmacol. Biochem. Behav.* **1976**, *5*, 111−116.

(6) Kalivas, P.; Horita, A. Thyrotropin-Releasing Hormone: Neurogenesis of Action in the Pentobarbital Narcotized Rat. *J. Pharmacol. Exp. Ther*. **1980**, *212*, 203−210.

(7) White, S. R.;Crane, G. K.; Rane, G. K.; Jackson, D. A. Thyrotropin-Releasing-Hormone (TRH) Effects on Spinal-Cord Neuronal Excitability. *Ann. N.Y. Acad. Sci*. **1989**, *553*, 337−350.

(8) Hashimoto, T.;Fukuda, N. Effect of Thyrotropin-Releasing-Hormone on the Neurologic Impairment in Rats with Spinal-Cord Injury-Treatment Starting 24-h and 7 Days after Injury. *Eur. J. Pharmacol*. **1991**, *203*, 25−32.

(9) Schröder, H.; Giacobini, E.; Struble, R.; Zilles, Z.; Maelicke, A. Nicotinic Cholinoceptive Neurons of the Frontal-Cortex are Reduced in Alzheimer's Disease. *Neurobiol. Aging* **1991**, *12*, 259−262.

(10) (a) Zlokovic, B. V.; Segal, M. B.; Begley, D. J.; Davson, H.; Rakic, L. Permeability of the Blood-Cerebrospinal Fluid and the Blood-Brain Barriers to Thyrotropin-Releasing Hormone. *Brain Res*. **1985**, *358*, 191−199. (b) Zlokovic, B. V.; Lipovac, M. N.; Begley, D. J.; Davson, H.; Rakic, L. Slow Penetration of Thyrotropin-Releasing Hormone Across the Blood-Brain Barrier of an In Situ Perfused Guinea Pig Brain. *J. Neurochem*. **1988**, *51*, 252−257.

(11) Meisenberg, G.; Simmons, W. Peptides and the Blood Brain Barrier. *Life Sci.* **1983**, *32*, 2611−2623.

(12) Szirtes, T.; Kisfaludy, L.; Palosi, E.; Szporny, L. Synthesis of Thyrotropin-Releasing Hormone Analogues. I. Complete Dissociation of Central Nervous System Effects from Thyrotropin-Releasing Activity. *J. Med. Chem.* **1984**, *27*, 741−745.

(13) (a) Kroll, R. A.; Neuwelt, E. A. Outwitting the Blood-Brain Barrier for Therapeutic Purposes: Osmotic Opening and Other Means. *Neurosurgery* **1998**, *42*, 1083−1099. (b) Fortin, D. Altering the properties of the blood-brain barrier: disruption and permeabilization. In *Progress in Drug Research;* Prokai, L., Prokai-Tatrai, K., Eds.; Birkhäuser Verlag: Basel, 2003; Vol. 61, p 127.

(14) (a) Prokai, L. Delivery of Peptides into the Central Nervous System. *Drug Discovery Today* **1996**, *1*, 161−167. (b) Prokai, L. Peptide Delivery into the Central Nervous System: Invasive Physiological and Chemical Approaches. *Exp. Opin. Ther. Pat.* **1997**, *7*, 233−245. (c) Prokai, L.; Prokai-Tatrai, K. Metabolism-Based Drug Design and Drug Targeting. *Pharm. Sci. Technol. Today* **1999**, *2*, 457−463. (d) Prokai-Tatrai, K.; Prokai, L. Modifying Peptide Properties by Prodrug Design for Enhanced Transport into the CNS. In *Progress in Drug Research;* Prokai, L., Prokai-Tatrai, K., Eds.; Birkhäuser Verlag: Basel, 2003; Vol. 61, p 155.

(15) Anderson, B. D. Prodrugs for Improved CNS Delivery. *Adv. Drug Del. Rev*. **1996**, *19*, 171−202.

(16) Prokai, L.; Prokai-Tatrai, K.; Bodor, N. Targeting Drugs to the Brain by Redox Chemical Delivery Systems. *Med. Res. Rev*. **2000**, *20*, 367−416 and references therein.

(17) Prokai, L.; Prokai-Tatrai, K.; Ouyang, X.; Kim, H. S.; Wu, W. M.; Zharikova, A. D.; Bodor, N. Metabolism-Based Brain-Targeting System for a Thyrotropin-Releasing Hormone Analogue. *J. Med. Chem.* **1999**, *42*, 4563−4571.

(18) Prokai-Tatrai, K.; Perjesi, P.; Zharikova, A. D.; Li, X.; Prokai, L. Design, Synthesis, and Biological Evaluation of Novel, Centrally-Acting Thyrotropin-Releasing Hormone Analogues. *Bioorg. Med. Chem. Lett*. **2002**, *12*, 2171−2174.

(19) Rivier, J.; Burgus, R.; Vale, W.; Ling, N.; Monahan, M. Synthetic Thyrotropin-Releasing Factor Analogs. 3. Effect of Replacement or Modification of Histidine Residue on Biological-Activity. *J. Med. Chem*. **1972**, *15*, 479−451.

(20) Bycroft, B. W.; Chan, W. C.; Chabra, S. R.; Hone, N. D. A Novel Lysine-Protecting Procedure for Continuous-Flow Solid-Phase Synthesis of Branched Peptides. *J. Chem. Soc., Chem. Commun*. **1993**, 778−779.

(21) Aletras, A.; Barlos, K.; Gatos, D.; Koutsogianni, S.; Mamos, P. Preparation of the Very Acid-Sensitive Fmoc-Lys(Mtt)-OH−Application in the Synthesis of Side-Chain to Side-Chain Cyclic-Peptides and Oligolysine Cores Suitable for the Solid-Phase Assembly of MAPS and TASP. *Int. J. Pept. Protein Res*. **1995**, *45*, 488−496.

(22) Augustyns, K.; Kraas, W.; Jung, G. Investigation on the Stability of the Dde Protecting Group Used in Peptide Synthesis: Migration to an Unprotected Lysine. *J. Pept. Res.* **1998**, *51*, 127−133.

(23) Eda,. M. E.; Kurth, M. J. Polymer Site-Site Interactions: Mechanistic Implication in the Solid-Phase Zincke Reaction. *J. Chem. Soc., Chem. Commun*. **2001**, 723−724

(24) Ong, S. W.; Liu, H. L.; Pidgeon, C. Immobilized Artificial-Membrane Chromatography: Measurements of Membrane Partition Coefficient and Predicting Drug Membrane Permeability. *J. Chromatogr. A* **1996**, *728*, 113−128.

(25) (a) Braddy, A. C.; Janaky, T.; Prokai, L. Immobilized Artificial Membrane Chromatography Coupled with Atmospheric Pressure Ionization Mass Spectrometry. *J. Chromatogr. A* **2002**, *966*, 81−87. (b) Prokai, L.; Prokai-Tatrai, K.; Zharikova, A. D.; Li, X. X.; Rocca, J. R. Combinatorial Lead Optimization of a Neuropeptide FF Antagonist. *J. Med. Chem*. **2001**, *44*, 1623−1626.

(26) An atom fragment method implemented in the molecular modeling package HyperChem version 6.0 (Hypercube, Gainesville, FL): Ghose, A. K.; Pritchett, A.; Crippen, G. M. Atomic Physicochemical Parameters for 3-Dimensional Structure Directed Quantitative Structure−Activity-Relationships. 3. Modeling Hydrophobic Interactions. *J. Comput. Chem*. **1988**, *9*, 80−90.

(27) Semiempirical quantum chemical (AM1) approach: Bodor, N.; Gabanyi, Z.; Wong, C. K. A New Method for the Estimation of Partition-Coefficient. *J. Am. Chem. Soc.* **1989**, *111*, 3783−3786.

(28) Molecular-volume based method: Buchwald, P.; Bodor, N. Octanol-Water Partition of Nonzwitterionic Peptides: Predictive Power of a Molecular Size-Based Model. *Proteins* **1998**, *30*, 86−99.

(29) Bundgaard, H.; Møss, J. Prodrugs of Peptides. 6. Bioreversible Derivatives of Thyrotropin-Releasing-Hormone (TRH) with Increased Lipophilicity and Resistance to Cleavage by the TRH-Specific Serum Enzyme. *Pharm. Res.* **1990**, *7*, 885−892.

(30) Prokai, L.; Zharikova, A. D. Neuropharmacodynamic Evaluation of the Centrally Active Thyrotropin-Releasing Hormone [Leu^2]TRH and its Chemical Brain-Targeting System. *Brain Res.* **2002**, *952*, 268−274.

(31) Prokai, L.; Zharikova, A. D.; Janaky, T.; Li, X. X.; Braddy, A. C.; Perjesi, P.; Matveeva, L.; Powell, D. H.; Prokai-Tatrai, K. Integration of Mass Spectrometry into Early-Phase Discovery and Development of Central Nervous System Agents. *J. Mass Spectrom*. **2001**, *36*, 1211−1219.
(32) Stewart, B. H.; Chung, F. Y.; Tait, B.; John, C.; Chan, O. H. Hydrophobicity of HIV Protease Inhibitor by Immobilized Artificial Membrane Chromatography: Application and Significance to Drug Transport. *Pharm. Res*. **1998**, *15*, 1401−1406.
(33) Reichel, A.; Begley, D. J. Potential of Immobilized Artificial Membranes for Predicting Drug Penetration across the Blood-Brain Barrier. *Pharm. Res*. **1998**, *15*, 1270−1274.
(34) Hansch, C.; Björkroth, J. P.; Leo, A. Hydrophobicity and Central Nervous System Agents: On the Principle of Minimal Hydrophobicity in Drug Design. *J. Pharm. Sci.* **1987**, *76*, 663−687.
(35) Cornford, E. M.; Braun, L. D.; Oldendorf, W. H.; Hill, M. A. Comparison of Lipid-Mediated Blood-Brain-Barrier Penetrability in Neonates and Adults. *Am. J. Physiol.* **1982**, *243*, C161−C168.
(36) Kanthimathi, T.; Hughes, L.; Subramanian, S. The Solution Structure of TRH−A ^{1}H-NMR Reinvestigation. *Magn. Reson. Chem*. **1995**, *34*, 283−88.
(37) (a) Burt, D. R.; Snyder, S. H. Thyrotropin Releasing Hormone (TRH): Apparent Receptor Binding in Rat Brain Membranes. *Brain Res*. **1975**, *93*, 309−328. (b) Simasko, S. K.; Horita, A. Characterization and Distribution of ^{3}H-(3MeHis^{2})Thyrotropin Releasing Hormone Receptors in Rat Brain. *Life Sci.* **1982**, *30*, 1793−1799.

JM020531T